Polymer Chemistry

PAPER

View Article Online
View Journal | View Issue

Cite this: *Polym. Chem.*, 2014, **5**, 3697

Macromolecular structure evolution toward giant molecules of complex structure: tandem synthesis of asymmetric giant gemini surfactants†

Hao Su,[a] Yiwen Li,*[a] Kan Yue,[a] Zhao Wang,[a] Pengtao Lu,[a] Xueyan Feng,[a] Xue-Hui Dong,[a] Shuo Zhang,[a] Stephen Z. D. Cheng*[a] and Wen-Bin Zhang*[ab]

Received 23rd January 2014
Accepted 17th February 2014

DOI: 10.1039/c4py00107a

www.rsc.org/polymers

Precise control of primary chemical structures, especially those of complex structures, is a prerequisite to understand the structure–property relationships of functional macromolecules. In this article, we report the rational design and tandem synthesis of three asymmetric giant gemini surfactants (AGGSs) of complex macromolecular structures based on polyhedral oligomeric silsesquioxane (POSS). In two cascading processes (typically within 5 hours), AGGSs can be synthesized where the length of the two polymer tails and the identity of the two POSS heads can be independently controlled and systematically varied. It represents a convenient, efficient, and modular way to prepare giant molecules with rigorous structural precision in only a few steps. This study expands the scope of synthetically available giant surfactants and facilitates further structural evolution toward even more complex macromolecules.

Introduction

Diverse macromolecular structures and their distinct three-dimensional shapes have played a critical role in the field of nanotechnology and attracted considerable attention in recent years.[1,2] By accurately controlling the chemical structure and functionality of polymers, chemists may develop the ability to predict and design the soft material properties.[2] For example, functions of many biomacromolecules (*i.e.* proteins or nucleic acids) are a direct consequence of the precise sequences of monomers and the resulting primary, secondary, tertiary and quaternary structures across over a broad length scale. However, synthetic polymers often lack the proper structural complexity desired for hierarchical structures and material functional controls. In fact, the rapid and precise synthesis of synthetic polymers with complex macromolecular architectures remains a grand challenge so far.[1,3,4]

The emergence of giant molecules provides new opportunities to achieve exquisite "precision" in structure control *via* modular, robust, and efficient chemistries.[5] A giant molecule describes the precisely defined macromolecules made from molecular nanoparticle subunits or their conjugates with other molecular nano-building blocks.[5] Among them, giant surfactants consist of polymer-tethered molecular nanoparticles, which capture the essential structural features of small-molecular surfactants with amplified sizes of several nanometers. Additionally, giant surfactants are also attractive as advanced functional materials by virtue of their capability to self-assemble into supramolecular structures with sub-10 nm feature sizes.[6,7] This class of unique macromolecules bridges the gap between small-molecular surfactants and block copolymers, and possesses a duality of both in terms of their self-assembly behaviors in the bulk and in solution.[6,7] In recent years, various types of giant surfactants have been designed and synthesized in analogy to their small-molecule counterparts, such as giant lipids,[8,9] giant gemini surfactants,[10,11] giant bola-form surfactants,[11] and multi-headed/multi-tailed giant surfactants.[11,12] The series of molecular design in giant surfactants also denotes an evolution toward complex macromolecular structures.

A few effective synthetic methodologies have been developed to facilitate the exact positioning of functionalities onto the nanoparticle's surface for subsequent integration with polymers and/or other molecular moieties.[5–7,13] So far, most of the efforts toward giant surfactants have focused on the introduction of functional polyhedral oligomeric silsesquioxane (POSS) nanoparticles as the head, since it allows precise control of shape, symmetry, number of tethered chains and localization of functional groups on the surface.[14–20] Tremendous success of connecting different types of tails onto the chemical functionalized POSS heads has been achieved by both "grafting-

[a]*Department of Polymer Science, College of Polymer Science and Polymer Engineering, The University of Akron, Akron, Ohio 44325-3909, USA. E-mail: yl48@zips.uakron.edu; wenbin@pku.edu.cn; scheng@uakron.edu; Fax: + 1 330 972 8626; +1 330 972 8626; Tel: +1 330 256 9458; +1 330 972 6931*

[b]*Key Laboratory of Polymer Chemistry and Physics of Ministry of Education, College of Chemistry and Molecular Engineering, Center for Soft Matter Science and Engineering, Peking University, Beijing 100871, P. R. China. Fax: + 86 10 6275 1708; Tel: +86 10 6275 2394*

† Electronic supplementary information (ESI) available: Details of characterization data including the synthesis and characterization of the compounds. See DOI: 10.1039/c4py00107a

from"[8,21] and "grafting-onto" strategies.[9,11,12,22] Since the former strategy lacks generality in view of the compatibility between the polymerization mechanism and functional groups on the POSS head,[8] the latter "grafting-onto" strategy seems to be a more robust approach for precision synthesis.[22]

"Click" chemistry fits well into the "grafting-onto" strategy since it guarantees near quantitative coupling.[5] In the "click" toolbox Cu(I)-catalyzed [3 + 2] azide-alkyne cycloaddition (CuAAC),[23] strain-promoted azide-alkyne cycloaddition (SPAAC),[24,25] thiol-ene "click" coupling (TECC) reaction[26–29] and oxime ligation are the most commonly used ones.[30,31] Combinations of these "click" reactions in either a sequential fashion or a one-pot process have been proven to be powerful in generating complex macromolecular structures. For example, our group has demonstrated a sequential triple "click" chemistry methodology based on the consecutive SPAAC, CuAAC, and TECC reactions in the preparation of POSS-based multi-headed/multi-tailed giant surfactants[12] and later adapted it to a one-pot synthesis of single-tailed and asymmetric multi-tailed giant surfactants.[9]

Gemini surfactants are perhaps one of the most commonly studied surfactants during the past decade.[32–35] They are so-called "gemini" since these amphiphilic compounds consist of two conventional surfactant subunits connected together *via* a spacer.[32] This class of materials often possesses high surface activities and displays unusual aggregation properties in solution.[32] Considerable efforts have been devoted to the design and synthesis of various asymmetric gemini surfactants (AGSs) (a.k.a. heterogemini or heterodimeric surfactants) made up of two different amphiphilic molecules.[36] It was found that the molecular asymmetry of AGSs as well as the total length of hydrophobic chains could significantly influence their micellization process.[37]

The design and synthesis of giant gemini surfactants have also been attempted. We have previously shown that the spacer length could greatly affect the solution self-assembly behaviors of symmetric giant gemini surfactants containing two carboxylic acid-functionalized POSS (APOSS) and two identical polystyrene (PS) tails.[10] It has been found that giant gemini surfactants with longer spacers exhibited a more stretched PS tail conformation in their micellar cores. To further facilitate molecular structural evolution by increasing the macromolecular complexity of giant surfactants, we direct our efforts on the precise construction of various asymmetric giant gemini surfactants (AGGSs) and on a systematic investigation of their self-assembly behaviors and structure–property relationships (Scheme 1). Notably, if we consider the functional POSS cage as one polymeric block, the corresponding POSS-based AGGSs could perhaps be viewed as a class of unique H-shape star block polymers.[38,39] While their self-assembly behaviors are of great interest, the synthesis of such complex structures presents an immense challenge, typically involving multi-step (>5 steps) synthesis and extensive purification.[9]

In this article, we report a tandem synthesis approach toward giant surfactants of complex structure from common precursors in just two steps and typically within 5 hours (Scheme 2). The fractal synthesis strategy takes advantage of the "click" adaptor so that each intermediate giant molecule in the sequential "click" approach may be used as a versatile building block for the further construction of macromolecular structures with higher complexity. Three types of AGGSs have been synthesized and both the polymer tail compositions and POSS surface functionalities could be precisely controlled and independently tuned.

Experimental section

Chemicals and solvents

The styrene monomer (Aldrich, 99%) was purified by distillation from calcium hydride under reduced pressure prior to use. Tetrahydrofuran (THF, Certified ACS, EM Science), methanol (Fisher Scientific, reagent grade), ethyl acetate (Fisher Scientific), toluene (Certified ACS), dichloromethane (Certified ACS), chloroform (Certified ACS), *N*,*N*-dimethylformamide (DMF, Sigma-Aldrich, anhydrous 99.8%) and hexanes (Certified ACS) were used after distillation. Cuprous bromide (CuBr, Aldrich, 98%) was freshly purified by stirring in acetic acid overnight, washed with acetone, and dried in vacuum. 2-Mercaptoacetic acid (Aldrich, >98%) was distilled under reduced pressure before use. Octavinyl POSS (VPOSS, Hybrid Plastics, >97%), *N*,*N*,*N*′,*N*″,*N*″-pentamethyldiethylene-triamine (PMDETA, Aldrich, 99%), 4-formylbenzoic acid (Aldrich, 97%), 2-bromoisobutyryl bromide (Aldrich, 98%), ethylene glycol (Aldrich, anhydrous, 99.8%), 2-hydroxyethyl 2-bromoisobutyrate (Aldrich, 95%), 4-(bromomethyl)benzoic acid (Sigma, 97%), (boc-aminooxy) acetic acid (Aldrich, 98%), 2,2-dimethoxy-2-phenylacetophenone (DMPA, Acros Organics, 99%), 1-thioglycerol (Sigma, >99%), *N*,*N*′-diisopropylcarbodiimide (DIPC, Acros Organics, 99%), 4-(dimethylamino) pyridine (DMAP, Aldrich, 99%), hydrogen chloride solution (Aldrich, 4 M in dioxane), sodium azide (Aldrich, >99%), succinic anhydride (Aldrich, >99%), *p*-toluenesulfonic acid (TsOH, Aldrich, 98.5%), and triethylamine (Et_3N, Aldrich, >99%) were used as received. Silica gel (VWR, 230–400 mesh) was activated by heating at 140 °C for 12 h. 4-(Dimethylamino) pyridinium toluene-*p*-sulfonate (DPTS),[10] *tert*-butyl mercaptoacetate,[40] 4-(azidomethyl)benzoic

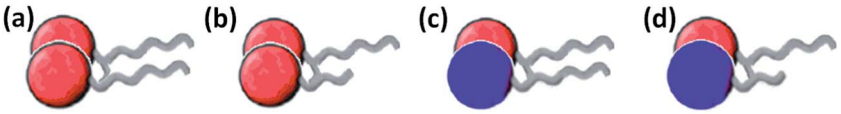

Scheme 1 Schematic illustrations of various kinds of giant gemini surfactants: (a) symmetric giant gemini surfactant; (b) asymmetric giant gemini surfactant with different polymer tails (AGGS1); (c) asymmetric giant gemini surfactant with different head groups (AGGS2); and (d) asymmetric giant gemini surfactant with different tails and heads (AGGS3).

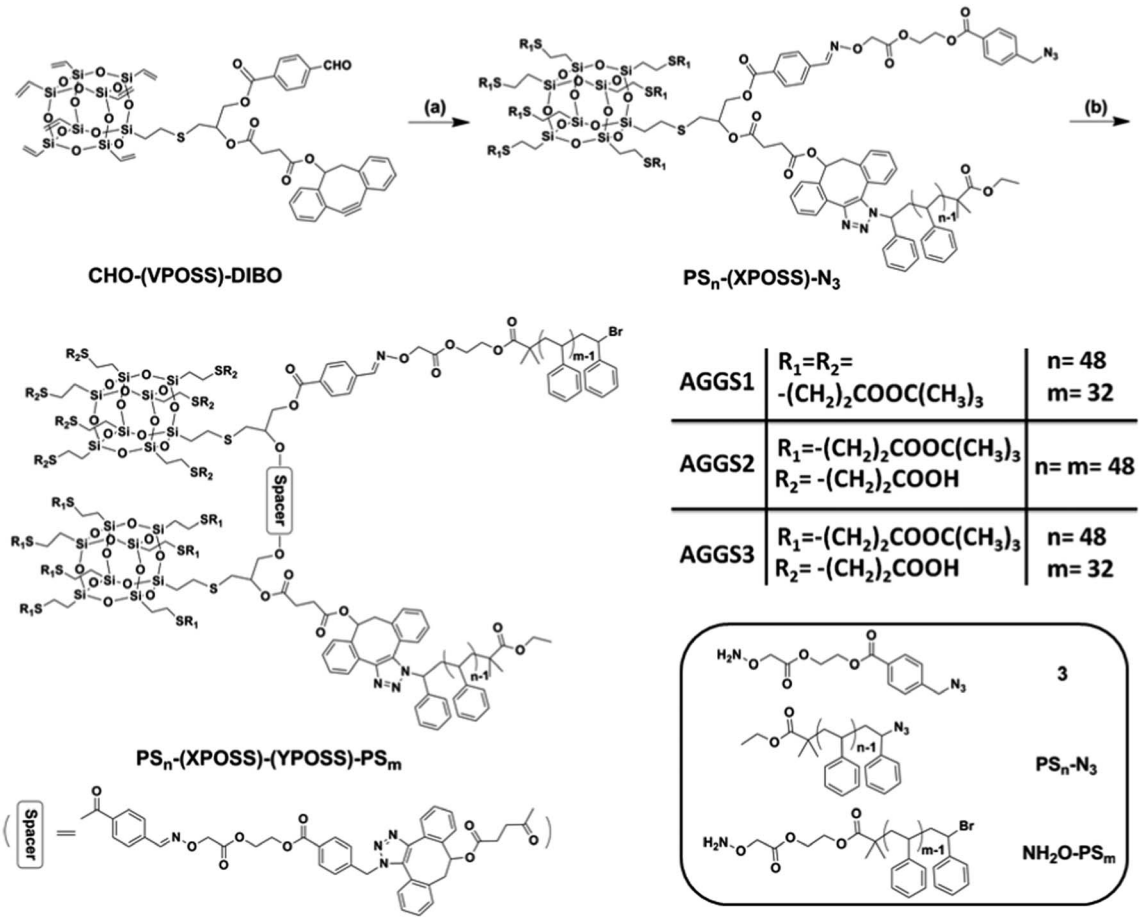

Scheme 2 General synthesis approaches for POSS-based AGGSs: (a): (i) PS_n–N_3, THF, 25 °C, 2 hours, without further purification; (ii) compound 3 (the "click" adaptor), TsOH, R_1-SH (*tert*-butyl mercaptoacetate), DMPA, THF, *hv*, 25 °C, 30 min, 82%. (b): (i) CHO-(VPOSS)-DIBO, THF, 25 °C, 2 hours, without further purification; (ii) NH_2O-PS_m, TsOH, R_2-SH (*tert*-butyl mercaptoacetate or 2-mercaptoacetic acid), DMPA, THF, *hv*, 25 °C, 30 min, 88% for AGGS1, 87% for AGGS1, and 84% for AGGS3.

acid,[41] azido-end-capped polystyrene (PS_n–N_3),[10] aminoxy-functionalized polystyrene (NH_2O-PS_m),[9] and CHO-(VPOSS)-DIBO[9] were synthesized as reported, respectively. The synthesis and characterization of compound 3 (the "click" adaptor) can be seen in the ESI.†

Materials characterization

Size exclusion chromatographic analyses (SEC) for the synthesized polymers were performed using a Waters 150-C Plus instrument equipped with three HR-Styragel columns [100 Å, mixed bed (50/500/10^3/10^4 Å), mixed bed (10^3, 10^4, 10^6 Å)], and a triple detector system. The three detectors included a differential refractometer (Waters 410), a differential viscometer (Viscotek 100), and a laser light scattering detector (Wyatt Technology, DAWN EOS, $\lambda = 670$ nm). THF was used as eluent with a flow rate of 1.0 mL min^{-1} at 30 °C.

All ^1H and ^{13}C NMR spectra were acquired in $CDCl_3$ (Aldrich, 99.8% D) utilizing Varian Mercury 300 NMR and 500 NMR spectrometers. The ^1H NMR spectra were referenced to the residual proton signals in the $CDCl_3$ at δ 7.27 ppm; while the ^{13}C NMR spectra were referenced to $^{13}CDCl_3$ at δ 77.00 ppm.

Infrared spectra were obtained on an Excalibur Series FT-IR spectrometer (DIGILAB, Randolph, MA) by casting films on KBr plates from solutions with subsequent drying at 40–50 °C. The spectroscopic data were processed using Win-IR software.

UV-Vis absorption spectra were collected using a Shimadzu 1750 UV-Vis spectrometer. The test sample was dissolved in chloroform at a concentration of 50 μmol mL^{-1} and transferred to a quartz cuvette for measurement.

Matrix-assisted laser desorption/ionization time-of-flight (MALDI-TOF) mass spectra were acquired on a Bruker Ultraflex-III TOF/TOF mass spectrometer (Bruker Daltonics, Inc., Billerica, MA) equipped with a Nd:YAG laser (355 nm). The spectra were measured in positive linear mode. The instrument was calibrated prior to each measurement with external PMMA or PS standards at the molecular weight under consideration. The compound *trans*-2-[3-(4-*tert*-butylphenyl)-2-methyl-2-propenylidene]-malononitrile (DCTB, Aldrich, >98%) served as the matrix and was prepared in $CHCl_3$ at a concentration of 20 mg mL^{-1}. The cationizing agent sodium trifluoroacetate or silver trifluoroacetate was prepared in MeOH–$CHCl_3$ (v/v = 1/3) at a concentration of 5 mg mL^{-1} or 10 mg mL^{-1}. The matrix and cationizing salt solutions were mixed in a ratio of 10/1 (v/v). All

samples were dissolved in $CHCl_3$ at a concentration of 10 mg mL^{-1}. The sample preparation followed the procedure of depositing 0.5 μL of the matrix and salt mixture on the wells of a 384-well ground-steel plate, allowing the spots to dry, depositing 0.5 μL of each sample on a spot of dry matrix/salt, and adding another 0.5 μL of matrix and salt mixture on top of the dry sample (sandwich method). After solvent evaporation, the plate was inserted into the MALDI mass spectrometer. The attenuation of the Nd:YAG laser was adjusted to minimize undesired polymer fragmentation and to maximize the sensitivity.

Electrospray ionization mass spectrometry (ESI MS) experiments were performed on a Waters Synapt HDMS instrument quadrupole/time-of-flight (Q/TOF) mass spectrometer (Waters, Milford, MA). The following ESI parameters were selected: ESI capillary voltage, 3.0 kV; sample cone voltage, 70 V; extraction cone voltage, 3.2 V; desolvation gas flow, 500 L h^{-1} (N_2); trap collision energy (CE), 6 eV; transfer CE, 4 eV; trap gas flow, 1.5 mL min^{-1} (Ar); sample flow rate, 5 μL min^{-1}; source temperature, 80 °C; desolvation temperature, 150 °C. The sprayed solutions were prepared by dissolving ~0.1 mg of sample in 1 mL of $CHCl_3$–MeOH (v/v, 50/50) containing 1% (v/v) NaTFA solution (1 mg mL^{-1} in MeOH). Data analysis was conducted with the MassLynx 4.1 program of Waters.

Thin-layer chromatographic analyses of the functionalized polymers were carried out by spotting samples on flexible silica gel plates (Selecto Scientific, Silica Gel 60, F-254 with a fluorescent indicator) and developing using toluene or its mixture with other polar solvents.

Synthetic procedures

PS_{48}-(*t*BAPOSS)-N_3. CHO-VPOSS-DIBO (100 mg, 0.0852 mmol) and PS_{48}–N_3 ($M_{n,NMR}$ = 5.1 kg mol^{-1}, 435 mg, 0.0852 mmol) were dissolved in 8 mL of THF. The mixture was stirred at room temperature for 2 hours, followed by the addition of compound 3 (25 mg, 0.0852 mmol), TsOH (5 mg, 0.0290 mmol), *tert*-butyl mercaptoacetate (126 mg, 0.852 mmol), and DMPA (2 mg, 0.005 mmol). The solution was then irradiated under UV 365 nm for 30 minutes, after which it was precipitated into cold methanol three times. The sample PS_{48}-(*t*BAPOSS)-N_3 was collected and dried under vacuum overnight to afford a white powder (531 mg; yield: 82%). SEC: M_n = 7.9 kg mol^{-1}, PDI = 1.02.

PS_{48}-(*t*BAPOSS)-(*t*BAPOSS)-PS_{32} (AGGS1). PS_{48}-(*t*BAPOSS)-N_3 ($M_{n,NMR}$ = 7.6 kg mol^{-1}, 150 mg, 0.0197 mmol) and CHO-VPOSS-DIBO (23 mg, 0.0197 mmol) were dissolved in 5 mL of THF. The mixture was stirred at room temperature for 2 hours, followed by the addition of NH_2O-PS_{32} ($M_{n,NMR}$ = 3.5 kg mol^{-1}, 69 mg, 0.0197 mmol), TsOH (5 mg, 0.0290 mmol), *tert*-butyl mercaptoacetate (29 mg, 0.197 mmol), and DMPA (2 mg, 0.005 mmol). The one pot solution was then irradiated under UV 365 nm for 30 minutes, after which it was precipitated into cold methanol solution three times. The sample PS_{48}-(*t*BAPOSS)-(*t*BAPOSS)-PS_{32} was collected and dried under vacuum overnight to afford a white powder (238 mg; yield: 88%). SEC: M_n = 14.1 kg mol^{-1}, PDI = 1.01.

PS_{48}-(*t*BAPOSS)-(APOSS)-PS_{48} (AGGS2). PS_{48}-(*t*BAPOSS)-N_3 ($M_{n,NMR}$ = 7.6 kg mol^{-1}, 150 mg, 0.0197 mmol) and CHO-VPOSS-DIBO (23 mg, 0.0197 mmol) were dissolved in 5 mL of THF. The mixture was stirred at room temperature for 2 hours, followed by the addition of NH_2O-PS_{48} ($M_{n,NMR}$ = 5.1 kg mol^{-1}, 100 mg, 0.0197 mmol), TsOH (5 mg, 0.0290 mmol), 2-mercaptoacetic acid (18 mg, 0.197 mmol), and DMPA (2 mg, 0.005 mmol). The solution was then irradiated under UV 365 nm for 30 minutes, after which it was precipitated into cold methanol three times. The sample PS_{48}-(*t*BAPOSS)-(APOSS)-PS_{48} was collected and dried under vacuum overnight to afford a white powder (250 mg; yield: 87%). SEC: M_n = 15.0 kg mol^{-1}, PDI = 1.10.

PS_{48}-(*t*BAPOSS)-(APOSS)-PS_{32} (AGGS3). PS_{48}-(*t*BAPOSS)-N_3 ($M_{n,NMR}$ = 7.6 kg mol^{-1}, 150 mg, 0.0197 mmol) and CHO-VPOSS-DIBO (23 mg, 0.0197 mmol) were dissolved in 5 mL of THF. The mixture was stirred at room temperature for 2 hours, followed by the addition of NH_2O-PS_{32} ($M_{n,NMR}$ = 3.5 kg mol^{-1}, 69 mg, 0.0197 mmol), TsOH (5 mg, 0.0290 mmol), 2-mercaptoacetic acid (18 mg, 0.197 mmol), and DMPA (2 mg, 0.005 mmol). The solution was then irradiated under UV 365 nm for 30 minutes, after which it was precipitated into cold methanol solution three times. The sample PS_{48}-(*t*BAPOSS)-(APOSS)-PS_{32} was collected and dried under vacuum overnight to afford a white powder (218 mg; yield: 84%). SEC: M_n = 14.4 kg mol^{-1}, PDI = 1.06.

Results and discussion

Molecular design of AGGSs

From a structural point of view, there are five molecular segments in an AGGS: two polymer tails, two heads and one spacer. To construct such giant surfactants in fewer steps, "click" chemistry seems to be an ideal tool since it is easy to perform, gives rise to the target products in high yields with limited or no byproducts, and is often unaffected by the nature of the functionalities being connected to each other.[4,42,43] For example, the combined utilization of multiple orthogonal "click" reactions has facilitated the rapid synthesis of multifunctional giant surfactants in a one-pot cascading process.[5]

The success of one-pot synthesis relies on the choice of suitable orthogonal "clickable" groups present on the precursor POSS cage. In our previous work, CHO-(VPOSS)-DIBO, an important precursor possessing three kinds of "click" functionalities (vinyl groups for TECC, a 4-dibenzocyclooctyne (DIBO) motif for SPAAC, and an aldehyde group for oxime ligation), has been proven to be a powerful precursor for the modular and facile one-pot synthesis of POSS-based multifunctional giant surfactants under mild conditions.[9] In this study, we continue to employ this readily accessible and highly versatile building block for further exploration of various AGGSs. Considering that CHO-(VPOSS)-DIBO could generate three different molecular segments at a time during the one-pot process, we are thus able to rapidly and efficiently construct AGGSs containing five distinct molecular species using sequential one-pot processes. Notably, the macromolecular intermediate equipped with a "click" adaptor after the first

one-pot process can be used as a new macromolecular "clickable" precursor for further functionalization into higher complexity.[11]

In the small-molecular AGS system, the asymmetry factor among heads or/and tails plays a significant role in determining the self-assembly behaviors of gemini surfactants in aqueous solution.[36] To create asymmetry in giant surfactants, we specifically design AGGSs possessing POSSs with different surface functionalities (*tert*-butyl mercaptoacetate functionalized POSS (*t*BAPOSS) *vs.* 2-mercaptoacetic acid functionalized POSS (APOSS)) or/and PS tails with different chain lengths (5.1 kg mol^{-1} *vs.* 3.5 kg mol^{-1}) (Scheme 2). To quantitatively describe the asymmetry factor, we propose to use A_{tail} ($0 \leq A_{\text{tail}} \leq 100\%$) of AGGSs based on the molecular weights of tails (M_{PS_1} and M_{PS_2}) as shown in eqn (1) since the two polymeric tails are of the same chemical compositions.

$$A_{\text{tail}} = \left| \frac{M_{\text{PS}_1} - M_{\text{PS}_2}}{M_{\text{PS}_1} + M_{\text{PS}_2}} \right| \times 100\% \quad (1)$$

It should also be noted that a similar definition would be difficult for the heads because they differ not only in molecular weights, but also in the identity of surface functional groups, the latter of which sometimes play an even more important role in self-assemblies. Nevertheless, similar to many other giant surfactants, the weight fraction of heads (W_{head}) or tails (W_{tail}) offers another important physics parameters to describe the asymmetry between heads and tails and to determine the self-assembly behaviors of AGGSs. They can be directly derived from eqn (2) and (3) as follows:

$$W_{\text{head}} = \frac{(M_{\text{XPOSS}} + M_{\text{YPOSS}})}{M_{\text{AGGS}}} \times 100\% \quad (2)$$

$$W_{\text{tail}} = \frac{(M_{\text{PS}_1} + M_{\text{PS}_2})}{M_{\text{AGGS}}} \times 100\% \quad (3)$$

where M_{XPOSS} and M_{YPOSS} are the molecular weights of each head and M_{AGGS} is the overall molecular weight.

In this work, *t*BAPOSS was selected as a model functionalized head in AGGS for the following reasons: (1) macromolecular structures rich in *tert*-butyl acetate *e.g.*, poly(*tert*-butyl acrylate, or P*t*BA) are usually immiscible with PS, and may lead to the formation of various nano-phase separated structures and patterns;[44–46] (2) multi-component macromolecules consisting of PS, poly(acrylic acid) (PAA), and P*t*BA or their analogues are intriguing subjects for the study of a broad range of self-assembled structures;[47,48] (3) facile tuning of head asymmetry can be achieved simply by controlled acidolysis that converts a *t*BAPOSS head into an APOSS head.[49]

A "clickable" giant surfactant

In Scheme 2, PS_{48}-(*t*BAPOSS)-N_3 was conveniently prepared by a sequential multi-step one-pot process. Taking advantage of the "molecular 'click' adaptor" (compound 3, see ESI†),[11] it could be used as a common "clickable" precursor for three different AGGSs after a second one-pot "click" process. In general, "click" adaptors are very useful for further expanding the scope of giant surfactants.[11] They usually contain two functional groups of completely orthogonal "click" reactivity (*e.g.*, CuAAC/SPAAC and oxime ligation in compound **3**), which can be employed to convert one"click" functionality to the other. The molecular structure and purity of compound **3** is supported by NMR techniques (see ESI†) and ESI MS spectrum (found 294.76 Da *versus* calcd 295.10 Da for $(M \cdot H)^+$).

The synthesis of PS_{48}-(*t*BAPOSS)-N_3 was directly performed by mixing equimolar amounts of CHO-(VPOSS)-DIBO and PS_{48}–N_3 ($M_{\text{n,NMR}}$ = 5.1 kg mol^{-1}, PDI = 1.08) in a common solvent (such as $CHCl_3$ or THF). The solution was then stirred at room temperature for about 2 hours. Without any further purification, the product was subject to further reaction with compound **3** (1.0 equiv.) and *tert*-butyl mercaptoacetate (10.0 equiv.) in the presence of *p*-toluenesulfonic acid (TsOH) (5 mg), and 2,2-dimethoxy-2-phenylacetophenone (DMPA) (2 mg) under the irradiation of UV 365 nm for 30 min. No chromatographic purification was involved, and all of the byproducts were conveniently removed by repeated precipitation into cold methanol.

Results from various molecular characterization techniques including ^{1}H NMR (Fig. 1a), ^{13}C NMR (Fig. S1a†), UV-vis (Fig. S2†), FT-IR (Fig. S3†), SEC (Fig. 2) and MALDI-TOF mass spectrometry (Fig. 3) fully support the successful preparation of the "clickable" giant surfactant. First, compared with NMR results of CHO-(VPOSS)-DIBO, the disappearance of the vinyl protons in the resonance range of δ (6.16–5.84) ppm in the ^{1}H NMR spectrum (Fig. 1a) and sp^2 carbon signals at δ 137.08 and 128.52 ppm (Fig. S1a†) in the ^{13}C NMR spectrum of PS_{48}-(*t*BAPOSS)-N_3 confirms the high efficiency of the thiol–ene functionalization of VPOSS cage. It convincingly agrees with the new characteristic resonances emerging in the range of δ 3.19 and 2.79 ppm in the ^{1}H NMR spectrum, which can be attributed to the protons of the newly-formed thiol ether bonds. Second, the success of the SPAAC reaction is revealed by the occurrence of two new distinct characteristic peaks at δ 6.26 and 6.11 ppm corresponding to the proton (a) on the DIBO in Fig. 1a, shifted from the single peak at δ 5.58 ppm in the ^{1}H NMR spectrum of CHO-(VPOSS)-DIBO.[9,12] In addition, the complete disappearance of the strong absorbance for strained alkyne in DIBO at ~306 nm in the UV-vis absorbance spectrum (Fig. S2a and S2b†) also indicates the near quantitative "click" cycloaddition.[9] Third, the characteristic peak at δ 10.09 ppm corresponding to free aldehyde protons in CHO-(VPOSS)-DIBO is completely missing in the new ^{1}H NMR spectrum of the resulting macromolecular precursor, suggesting the success of the oxime ligation reaction. The incorporation of the azido-functionalized spacer after the one-pot reaction can be demonstrated by both benzyl azide protons (c) at δ 4.40 ppm in the ^{1}H NMR spectrum of (Fig. 1a) and a strong characteristic vibrational band at around 2100 cm^{-1} for the azide group in the FT-IR spectrum (Fig. S3†). Moreover, the SEC overlay shows a single symmetric distribution for PS_{48}-(*t*BAPOSS)-N_3 (M_n = 7.9 kg mol^{-1}, PDI = 1.02) shifted to a lower retention volume relative to that of PS_{48}–N_3 (M_n = 5.2 kg mol^{-1}, PDI = 1.08) due to an increase in molecular weight (Fig. 2 and Table 1). Finally, in the MALDI-TOF mass spectrum (Fig. 3), a single narrow molecular weight

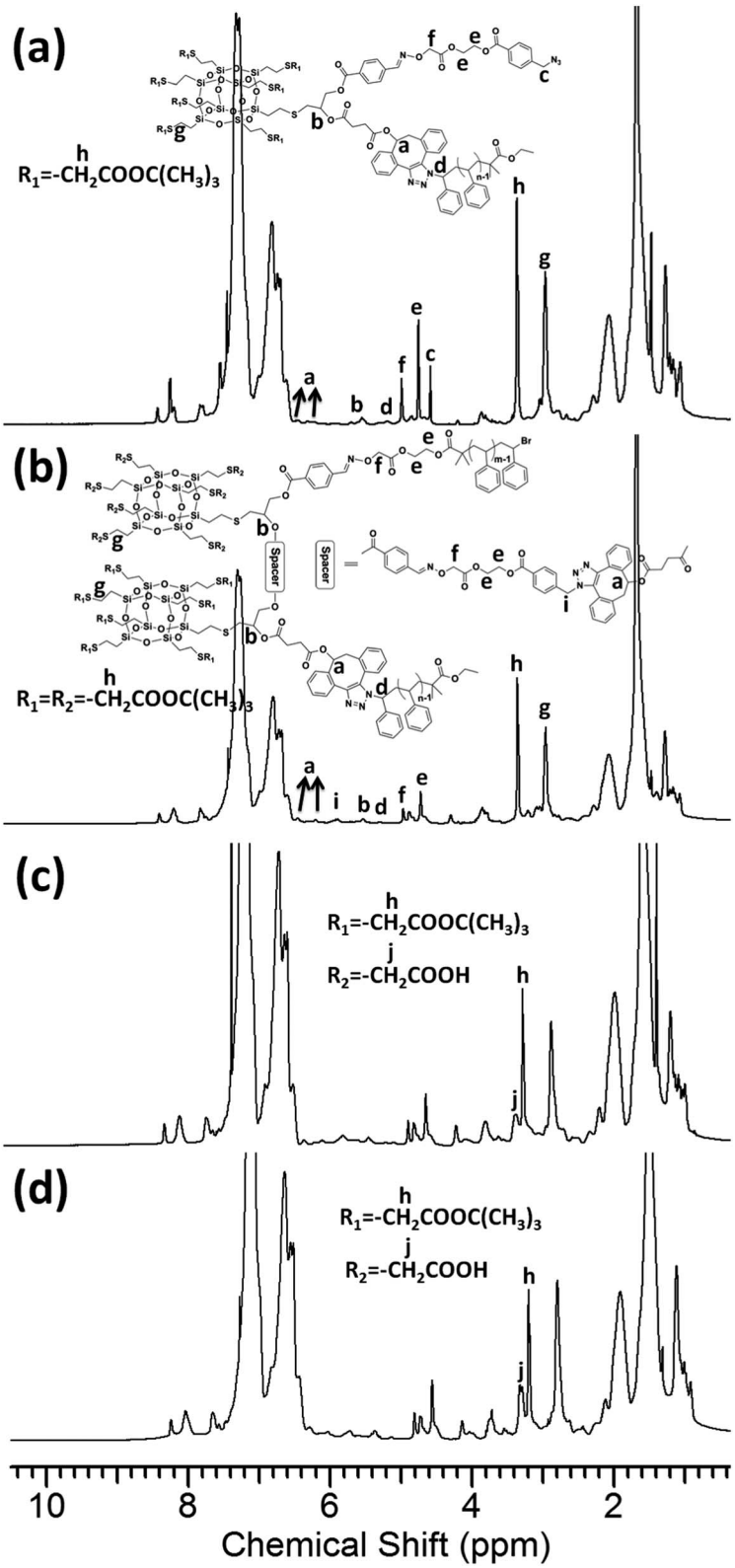

Fig. 1 ^{1}H NMR spectra of (a) PS_{48}-(*t*BAPOSS)-N_3, (b) PS_{48}-(*t*BAPOSS)-(*t*BAPOSS)-PS_{32}, (c) PS_{48}-(*t*BAPOSS)-(APOSS)-PS_{48}, and (d) PS_{48}-(*t*BAPOSS)-(APOSS)-PS_{32}.

distribution can be clearly observed under the positive linear mode despite the relatively high molecular weight of PS_{48}-(*t*BAPOSS)-N_3. Although monoisotopic resolution is not possible in this molecular weight range, the average molecular weights of the peaks match well with the calculated values (*e.g.*, for 46-mer with the formula of $C_{475}H_{525}N_5NaO_{39}S_8Si_8$, observed *m*/*z*

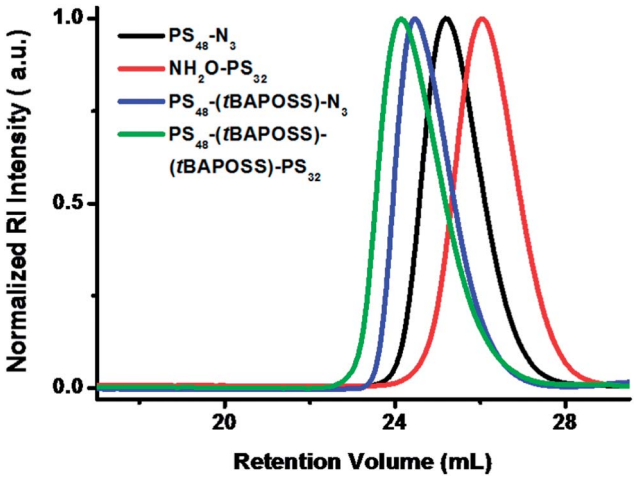

Fig. 2 SEC overlays for polymers: PS_{48}–N_3 (black curve), NH_2O-PS_{32} (red curve), PS_{48}-(*t*BAPOSS)-N_3 (blue curve), and PS_{48}-(*t*BAPOSS)-(*t*BAPOSS)-PS_{32} (green curve).

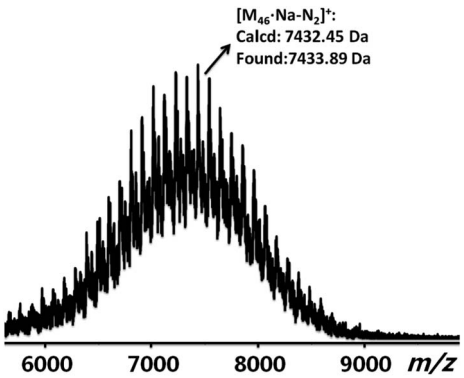

Fig. 3 MALDI-TOF mass spectra of PS_{48}-(*t*BAPOSS)-N_3. The full spectrum was obtained in positive linear mode.

7433.89 Da *vs.* calcd 7432.45 Da). Notably, PS_{48}-(*t*BAPOSS)-N_3 also holds the peak mass shift of $m/z = 2490.03$ relative to the precursor PS_{48}–N_3 ($[M_{46}\cdot Na–N_2]^+$) (4943.86 Da, see Fig. S4†), which corresponds to the precise "click" addition of one CHO-(VPOSS)-DIBO building block (1175.64 Da), one compound **3** (294.26 Da), and seven *tert*-butyl mercaptoacetate molecules (1037.56 Da), with the loss of one water molecule. Therefore, all the results obtained confirm the molecular structures and uniformity of the resulting intermediate product, a "clickable" giant surfactant.

Tandem synthesis of AGGSs

It is well-known from researches on structure–property relationships of small molecular AGSs that an asymmetric geometry may offer interesting characteristics in terms of self-assembly in solutions and at the interfaces.[36] For example, systematic tuning of the micellar interfacial curvatures can be achieved by varying different tail lengths in AGSs.[37,50] Oda and co-workers carefully correlate the micellar morphology and physical properties of the phases formed by gemini surfactants through adjusting the overall hydrophobic chain length and tail asymmetry.[37] In addition, Renouf *et al.* revealed that another small-molecular AGS, with distinct head groups but same tails, exhibited a critical micelle concentration (cmc) value below that of the corresponding symmetric gemini surfactants.[51] Therefore, it is of great interest to synthesize and study their counterparts in giant surfactants (Scheme 1). Considering the significance of several key structural elements, we may also need to pay more attention to similar factors in the AGGS system, such as W_{tail} (or W_{head}), and A_{tail}. It should be noted that the asymmetry could not be fully described by these parameters. AGGSs provide an even broader range of possibilities for topological variations and structural sophistication. Besides the two kinds of AGGSs mentioned above including AGGS1 with two polymer tails differing in chain lengths and two identical heads ($0 < A_{tail} < 100\%$), and AGGS2 having two distinct functional heads and two similar tails ($A_{tail} = 0$), it is nontrivial to further design and prepare new AGGS3 possessing two tails of different lengths and two distinct head groups ($0 < A_{tail} < 100\%$) inspired by the macromolecular structural evolution of giant molecules.

Subjecting PS_{48}-(*t*BAPOSS)-N_3 to the one-pot process with CHO-(VPOSS)-DIBO and another polymer tail conveniently affords a variety of different AGGSs. Herein, we demonstrate the ease of the tandem synthetic strategy by the construction of three AGGSs with tunable head groups and tails using a distinct polymer (NH_2O-PS_m) and another thiol ligand (R_2-SH). Although AGGSs might be prepared by our previously reported sequential "click" method, we always strive to achieve precision synthesis through the fewest steps possible, such as the two consecutive one-pot "click" processes.

Table 1 Summary of molecular characterization and physical parameters of products

Sample	$M_{n,NMR}$[a] (g mol^{-1})	$M_{n,SEC}$[b] (g mol^{-1})	$M_{w,SEC}$[c] (g mol^{-1})	PDI	W_{head}[d]	W_{tail}[e]	A_{tail}[f]
PS_{48}–N_3	5.1k	5.2k	5.6k	1.08	—	—	—
NH_2O-PS_{32}	3.5k	3.9k	4.3k	1.09	—	—	—
NH_2O-PS_{48}	5.1k	5.2k	5.5k	1.05	—	—	—
PS_{48}-(*t*BAPOSS)-N_3	7.6k	7.9k	8.1k	1.02	21.5%	67.1%	—
PS_{48}-(*t*BAPOSS)-(*t*BAPOSS)-PS_{32}	13.7k	14.1k	14.2k	1.01	23.9%	62.8%	18.6%
PS_{48}-(*t*BAPOSS)-(APOSS)-PS_{48}	14.6k	15.0k	16.5k	1.10	19.8%	69.9%	0
PS_{48}-(*t*BAPOSS)-(APOSS)-PS_{32}	13.2k	14.4k	15.3k	1.06	21.9%	65.2%	18.6%

[a] Molecular weight calculated based on ^{1}H NMR. [b] Molecular weight measured from SEC. [c] Molecular weight measured from SEC. [d] Weight fraction of heads calculated based on eqn (2). [e] Weight fraction of tails calculated based on eqn (3). [f] Asymmetry of tails calculated based on eqn (1).

First of all, the synthesis of model AGGS1, PS_{48}-(*t*BAPOSS)-(*t*BAPOSS)-PS_{32}, started by mixing equimolar amounts of macromolecular precursor, PS_{48}-(*t*BAPOSS)-N_3 ($M_{n,NMR}$ = 7.6 kg mol^{-1}, PDI = 1.02), and CHO-VPOSS-DIBO in a common solvent. The mixture was stirred at room temperature for about 2 hours, followed by the addition of amino-oxy chain-end functionalized PS tail 2 for AGGS1 (NH_2O-PS_{32}, $M_{n,NMR}$ = 3.5 kg mol^{-1}, PDI = 1.09), a functional thiol for the second POSS head modification (*tert*-butyl mercaptoacetate, 10.0 equiv.) and a few milligrams of TsOH and DMPA. The whole solution was then irradiated under UV 365 nm for about half an hour, and the final product was collected as a white powder in a good yield (~88%) after repeated precipitation into cold methanol.

Similar to PS_{48}-(*t*BAPOSS)-N_3, both ^{1}H (Fig. 1b) and ^{13}C NMR (Fig. S1b†) results confirm the complete consumption of the vinyl groups by TECC after the reaction by the disappearance of the corresponding proton and carbon peaks, respectively. In addition, the absence of aldehyde protons at δ 10.09 ppm in the ^{1}H NMR spectrum of PS_{48}-(*t*BAPOSS)-(*t*BAPOSS)-PS_{32} (Fig. 1b) also indicate the successful oxime ligation. Moreover, the disappearance of the strong characteristic vibrational band for the azide group at ~2100 cm^{-1} in the FT-IR spectrum (Fig. S3c†) as well as the absorbance for the DIBO motif at 306 nm in the UV-vis spectrum (Fig. S2c†) suggests the successful stoichiometric SPAAC reaction. This could also be supported by the complete shifting of resonance signals for the protons (c) adjacent to the azide group from δ 4.40 ppm to δ 5.75 ppm in the ^{1}H NMR spectrum (Fig. 1b). The increased overall molecular weight due to the incorporation of another two macromolecular segments during the one-pot process is also reflected by the clear shift in retention volume of PS_{48}-(*t*BAPOSS)-(*t*BAPOSS)-PS_{32} (M_n = 14.1 kg mol^{-1}, PDI = 1.01) compared with PS_{48}-(*t*BAPOSS)-N_3 (M_n = 7.9 kg mol^{-1}, PDI = 1.02) in the SEC overlay (Fig. 2). Although satisfactory MALDI-TOF mass spectra could not be obtained for this sample, probably due to its relatively high molecular weight and complex molecular structure, the precisely-defined structure of the product (AGGS1) can be validated by all other characterization techniques (W_{tail} = 62.8%, A_{tail} = 18.6%).

The synthetic approach for the model product of AGGS2, PS_{48}-(*t*BAPOSS)-(APOSS)-PS_{48}, again takes advantage of the one-pot "click" strategy by using a combination of several "click" reactions. The procedure is similar to the one for PS_{48}-(*t*BAPOSS)-(*t*BAPOSS)-PS_{32}, but using an amino-oxy chain-end functionalized PS of different molecular weights (NH_2O-PS_{48}, $M_{n,NMR}$ = 5.1 kg mol^{-1}, PDI = 1.05) and another functional thiol for the second POSS head (2-mercaptoacetic acid). The final product was fully characterized by various techniques including ^{1}H NMR (Fig. 1c), ^{13}C NMR (Fig. S1c†), UV-vis spectroscopy (Fig. S2†), FT-IR (Fig. S5†) and SEC (Fig. 4) to confirm the macromolecular structure and uniformity. Notably, the installation of the APOSS nanocage as the second head for AGGS2 is supported by the observation of the characteristic peak for protons (i) of (-CH_2COOH) at δ 3.32 ppm in the ^{1}H NMR spectrum (Fig. 1c) and a strong absorbance band at around 3300 cm^{-1} in the FT-IR spectrum FT-IR (Fig. S5b†). In addition, similar to the general characterization of PS_{48}-(*t*BAPOSS)-(*t*BAPOSS)-PS_{32}, the success of TECC, oxime ligation and SPAAC reactions during the one-pot synthetic process could be directly proved by the disappearance of the resonance peaks for vinyl protons and carbon atoms in the NMR spectra (Fig. 1c and S1c†), the absence of aldehyde proton resonance at δ 10.09 ppm in the ^{1}H NMR spectrum (Fig. 1c), and the loss of the vibrational band at ~2100 cm^{-1} in the FT-IR spectrum (Fig. S5†) as well as the absorbance peak at 306 nm in the UV-vis spectrum (Fig. S2†), respectively. Moreover, from the SEC overlay shown in Fig. 4, it is evident that the SEC trace of the final product, PS_{48}-(*t*BAPOSS)-(APOSS)-PS_{48} (M_n = 15.0 kg mol^{-1}, PDI = 1.10), shifts its peak position to a smaller retention volume after the one-pot "click" process. Therefore, it can be concluded that the model AGGS2 has been successfully synthesized by repeating the one-pot "click" methodology (W_{tail} = 69.9%).

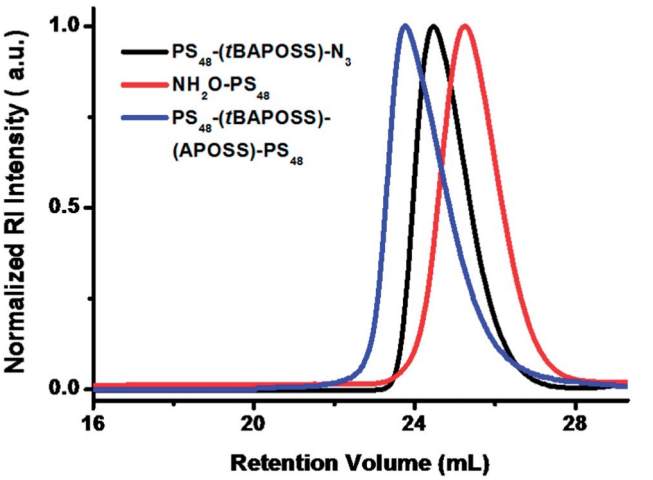

Fig. 4 SEC overlays for polymers: PS_{48}-(*t*BAPOSS)-N_3 (black curve), NH_2O-PS_{48} (red curve), and PS_{48}-(*t*BAPOSS)-(APOSS)-PS_{48} (blue curve).

Similarly, the synthesis of PS_{48}-(*t*BAPOSS)-(APOSS)-PS_{32} (model compound of AGGS3) could be simply conducted using a different thiol ligand (2-mercaptoacetic acid) for the second POSS head. The successful organization of distinct molecular segments into PS_{48}-(*t*BAPOSS)-(APOSS)-PS_{32} *via* different three types of "click" reactions was supported by ^{1}H NMR (Fig. 1d), ^{13}C NMR (Fig. S1d†), FT-IR (Fig. S5c†), and UV-vis spectra (Fig. S2e†). Furthermore, the SEC chromatogram of PS_{48}-(*t*BAPOSS)-(APOSS)-PS_{32} (Fig. 5) exhibits a monomodal, symmetric peak with a narrow molecular weight distribution (M_n = 14.4 kg mol^{-1}, PDI = 1.06). There is a clear shift in retention volume compared to that of PS_{48}-(*t*BAPOSS)-N_3 (M_n = 7.9 kg mol^{-1}, PDI = 1.02), consistent with the molecular weight increase as a result of the incorporation of new macromolecular blocks. All those results established the chemical structure and uniformity of the final product, and several important structural factors were also determined (W_{tail} = 65.2%, A_{tail} = 18.6%).

Notably, all the important structural elements (W_{head}, W_{tail}, and A_{tail}) in AGGSs can be facilely tuned during the tandem synthesis by using different polymers and functional thiols. No more synthetic steps or specific purification protocols are

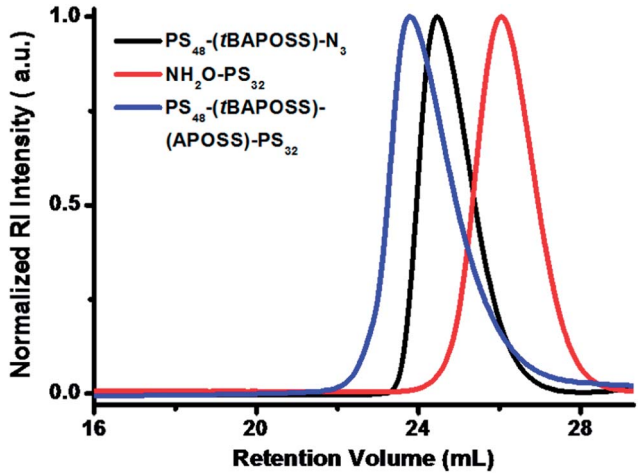

Fig. 5 SEC overlays for polymers: PS_{48}-(*t*BAPOSS)-N_3 (black curve), NH_2O-PS_{32} (red curve), and PS_{48}-(*t*BAPOSS)-(APOSS)-PS_{32} (blue curve).

required. Therefore, such a general and modular synthetic methodology enables the synthesis of a library of AGGSs for quantitative structure–property investigations. For example, by fixing W_{tail} but tuning A_{tail} values *via* introduction of two tails with different chain lengths, a series of topological isomers of AGGS1 may be obtained for a systematic study of their self-assembly behaviors.[9]

Conclusions

In summary, we have successfully developed three novel POSS-based AGGSs by using the tandem one-pot "click" methodology. The work demonstrates that this method can be adapted to prepare "clickable" giant surfactants using a "click" adaptor for subsequent tandem synthesis of AGGSs. The synthetic procedure was completed within 5 hours and the purification was achieved through repeated precipitation. Several important molecular parameters in AGGSs, such as overall molecular mass, surface functionalities of the nanoparticle, weight fraction of heads/tails, asymmetry of head/tail can be independently controlled and systematically varied. In general, this strategy not only provides an easy access to novel H-shape ABCDE star block copolymers, but also could be extended to allow a tandem "fractal" synthesis of diverse, complex POSS-based giant surfactants from modular building blocks for the systematic study of structure–property relationships. Echoing the evolution and increasing sophistication of giant-molecular structures, the development of such a simple, yet robust and precise synthetic protocol should be broadly applicable.

Acknowledgements

This work was supported by the National Science Foundation (DMR-0906898) and the Joint-Hope Education Foundation. We thank Ms Kai Guo and Prof. Chrys Wesdemiotis for their help with the MALDI-TOF and ESI mass characterization.

References

1 K. L. Wooley, J. S. Moore, C. Wu and Y. Yang, *Proc. Natl. Acad. Sci. U. S. A.*, 2000, **97**, 11147–11148.
2 C. J. Hawker and K. L. Wooley, *Science*, 2005, **309**, 1200–1205.
3 J. Zhang, M. E. Matta and M. A. Hillmyer, *ACS Macro Lett.*, 2012, **1**, 1383–1387.
4 R. K. Iha, K. L. Wooley, A. M. Nyström, D. J. Burked, M. J. Kade and C. J. Hawker, *Chem. Rev.*, 2009, **109**, 5620–5686.
5 W.-B. Zhang, X. Yu, C.-L. Wang, H.-J. Sun, I.-F. Hsieh, Y. Li, X.-H. Dong, K. Yue, R. M. Van Horn and S. Z. D. Cheng, *Macromolecules*, 2014, **47**, 1221–1239.
6 X. Yu, K. Yue, I.-F. Hsieh, Y. Li, X.-H. Dong, C. Liu, Y. Xin, H.-F. Wang, A.-C. Shi, G. R. Newkome, R.-M. Ho, E.-Q. Chen, W.-B. Zhang and S. Z. D. Cheng, *Proc. Natl. Acad. Sci. U. S. A.*, 2013, **110**, 10078–10083.
7 X. Yu, S. Zhong, X. Li, Y. Tu, S. Yang, R. M. Van Horn, C. Ni, D. J. Pochan, R. P. Quirk, C. Wesdemiotis, W.-B. Zhang and S. Z. D. Cheng, *J. Am. Chem. Soc.*, 2010, **132**, 16741–16744.
8 Y. Li, X.-H. Dong, K. Guo, Z. Wang, Z. Chen, C. Wesdemiotis, R. P. Quirk, W.-B. Zhang and S. Z. D. Cheng, *ACS Macro Lett.*, 2012, **1**, 834–839.
9 Y. Li, Z. Wang, J. Zheng, H. Su, F. Lin, K. Guo, X. Feng, C. Wesdemiotis, M. L. Becker, S. Z. D. Cheng and W.-B. Zhang, *ACS Macro Lett.*, 2013, **2**, 1026–1032.
10 Z. Wang, Y. Li, X.-H. Dong, X. Yu, K. Guo, H. Su, K. Yue, C. Wesdemiotis, S. Z. D. Cheng and W.-B. Zhang, *Chem. Sci.*, 2013, **4**, 1345–1352.
11 K. Yue, C. Liu, K. Guo, K. Wu, X.-H. Dong, H. Liu, M. Huang, C. Wesdemiotis, S. Z. D. Cheng and W.-B. Zhang, *Polym. Chem.*, 2013, **4**, 1056–1067.
12 H. Su, J. Zheng, Z. Wang, F. Lin, X. Feng, X.-H. Dong, M. L. Becker, S. Z. D. Cheng, W.-B. Zhang and Y. Li, *ACS Macro Lett.*, 2013, **2**, 645–650.
13 X.-H. Dong, W.-B. Zhang, Y. Li, M. Huang, S. Zhang, R. P. Quirk and S. Z. D. Cheng, *Polym. Chem.*, 2012, **3**, 124–134.
14 Y. Li, W.-B. Zhang, I.-F. Hsieh, G. Zhang, Y. Cao, X. Li, C. Wesdemiotis, B. Lotz, H. Xiong and S. Z. D. Cheng, *J. Am. Chem. Soc.*, 2011, **133**, 10712–10715.
15 D. B. Cordes, P. D. Lickiss and F. Rataboul, *Chem. Rev.*, 2010, **110**, 2081–2173.
16 S.-W. Kuo and F.-C. Chang, *Prog. Polym. Sci.*, 2011, **36**, 1649–1696.
17 M. F. Roll, M. Z. Asuncion, J. Kampf and R. M. Laine, *ACS Nano*, 2008, **2**, 320–326.
18 F. Wang, X. Lu and C. He, *J. Mater. Chem.*, 2011, **21**, 2775–2782.
19 K. Tanaka and Y. Chujo, *J. Mater. Chem.*, 2012, **22**, 1733–1746.
20 Y. Li, K. Guo, H. Su, X. Li, X. Feng, Z. Wang, W. Zhang, S. Zhu, C. Wesdemiotis, S. Z. D. Cheng and W.-B. Zhang, *Chem. Sci.*, 2014, **5**, 1046–1053.

21 W.-B. Zhang, Y. Li, X. Li, X. Dong, X. Yu, C.-L. Wang, C. Wesdemiotis, R. P. Quirk and S. Z. D. Cheng, *Macromolecules*, 2011, **44**, 2589–2596.
22 K. Yue, C. Liu, K. Guo, X. Yu, M. Huang, Y. Li, C. Wesdemiotis, S. Z. D. Cheng and W.-B. Zhang, *Macromolecules*, 2012, **45**, 8126–8134.
23 H. C. Kolb, M. G. Finn and K. B. Sharpless, *Angew. Chem., Int. Ed.*, 2001, **40**, 2004–2021.
24 J.-F. Lutz, *Angew. Chem., Int. Ed.*, 2008, **47**, 2182–2184.
25 J. Zheng, L. A. Smith Callahan, J. Hao, K. Guo, C. Wesdemiotis, R. A. Weiss and M. L. Becker, *ACS Macro Lett.*, 2012, **1**, 1071–1073.
26 A. B. Lowe, *Polym. Chem.*, 2010, **1**, 17–36.
27 Y. Li, W.-B. Zhang, J. E. Janoski, X. Li, X. Dong, C. Wesdemiotis, R. P. Quirk and S. Z. D. Cheng, *Macromolecules*, 2011, **44**, 3328–3337.
28 C. E. Hoyle and C. N. Bowman, *Angew. Chem., Int. Ed.*, 2010, **49**, 1540–1573.
29 M. J. Kade, D. J. Burke and C. J. Hawker, *J. Polym. Sci., Part A: Polym. Chem.*, 2010, **48**, 743–750.
30 K. L. Heredia, Z. P. Tolstyka and H. D. Maynard, *Macromolecules*, 2007, **40**, 4772–4779.
31 A. Dirksen and P. E. Dawson, *Bioconjugate Chem.*, 2008, **19**, 2543–2548.
32 F. M. Menger and J. S. Keiper, *Angew. Chem., Int. Ed.*, 2000, **39**, 1906–1920.
33 R. Zana, *J. Colloid Interface Sci.*, 2002, **248**, 203–220.
34 S. Karaborni, K. Esselink, P. A. J. Hilbers, B. Smit, J. Karthäuser, N. M. Van Os and R. Zana, *Science*, 1994, **266**, 254–256.
35 G. P. Sorenson, K. L. Coppage and M. K. Mahanthappa, *J. Am. Chem. Soc.*, 2011, **133**, 14928–14931.
36 E.-O. Alami and K. Holmberg, *Adv. Colloid Interface Sci.*, 2003, **100–102**, 13–46.
37 R. Oda, I. Huc and S. J. Candau, *Chem. Commun.*, 1997, 2105–2106.
38 A. Jabbarzadeh, J. D. Atkinson and R. I. Tanner, *Macromolecules*, 2003, **36**, 5020–5031.
39 C. Detrembleur, A. Debuigne, O. Altintas, M. Conradi, E. H. H. Wong, C. Jérôme, C. J. Barner-Kowollik and T. Junkers, *Polym. Chem.*, 2012, **3**, 135–147.
40 S. R. Woulfe and M. J. Miller, *J. Org. Chem.*, 1986, **51**, 3133–3139.
41 J. S. Foot, F. E. Lui and R. Kluger, *Chem. Commun.*, 2009, 7315–7317.
42 W. H. Binder and R. Sachsenhofer, *Macromol. Rapid Commun.*, 2007, **28**, 15–54.
43 Y. Zhao, G.-C. Kuang, R. J. Clark and L. Zhu, *Org. Lett.*, 2012, **14**, 2590–2593.
44 S. Nagarajan, T. P. Russell and J. J. Watkins, *Adv. Funct. Mater.*, 2009, **19**, 2728–2734.
45 B. Zhao and L. Zhu, *J. Am. Chem. Soc.*, 2006, **128**, 4574–4575.
46 X. Jiang, G. Zhong, J. M. Horton, N. Jin, L. Zhu and B. Zhao, *Macromolecules*, 2010, **43**, 5387–5395.
47 D. J. Pochan, Z. Chen, H. Cui, K. Hales, K. Qi and K. L. Wooley, *Science*, 2004, **306**, 94–97.
48 H. Cui, Z. Chen, S. Zhong, K. L. Wooley and D. J. Pochan, *Science*, 2007, **317**, 647–650.
49 W. F. DeGrado and E. T. Kaiser, *J. Org. Chem.*, 1982, **47**, 3258–3261.
50 G. Bai, J. Wang, Y. Wang, H. Yan and R. K. Thomas, *J. Phys. Chem. B*, 2002, **106**, 6614–6616.
51 P. Renouf, C. Mioskowski, L. Lebeau, D. Hebrault and J.-R. Desmurs, *Tetrahedron Lett.*, 1998, **39**, 1357–1360.

